Simultaneous interpolation and denoising based on a modified thresholding method

JINGJIE CAO[1,2], SHANGXU WANG[1] AND WENQUAN LIANG[3]

1 State Key Laboratory of Petroleum Resources and Prospecting, China University of Petroleum (Beijing), 102249 Beijing, China (cao18601861@163.com)

2 Hebei GEO University, Shijiazhuang, 050031 Hebei,China

3 Longyan University, Longyan, 364012 Fujian,China

Received: April 29, 2019; Revised: July 28, 2019; Accepted: September 7, 2019

ABSTRACT

Seismic interpolation can provide complete data for some multichannel processing techniques such as time lapse imaging and wave equation migration. However, field seismic data often contains random noise and noisy data interpolation is a challenging task. A traditional method applies interpolation and denoising separately, but this needs two workflows. Simultaneous interpolation and denoising combines interpolation and denoising in one workflow and can also get acceptable results. Most existing interpolation methods can only recover missing traces but fail to attenuate noise in sampled traces. In this study, a novel thresholding strategy is proposed to remove the noise in the sampled traces and meanwhile recover missing traces during interpolation. For each iteration, the residual is multiplied by a weighting factor and then added to the iterative solution, after which the sum in the transformed domain is calculated using the thresholding operation to update the iterative solution. To ensure that the interpolation and denoising results are robust, the exponential method was chosen to reduce the threshold values in small quantities. The curvelet transform was used as sparse representation and three interpolation methods were chosen as benchmarks. Three numerical tests results proved the effectiveness of the proposed method on removing noise in the sampled traces when the minimum threshold values are correctly chosen.

Keywords: interpolation, sparsity, seismic inversion, noise, thresholding method

1. INTRODUCTION

Field seismic signals have always been under-sampled across spatial areas due to limitations of high costs, topography, feathering, and so on. Seismic data violating the Nyquist/Shannon sampling theory may affect the quality of some crucial multichannel techniques such as wave-equation migration (*Yao et al., 2016, 2018*), time-lapse seismic imaging (*Smith et al., 2012*), seismic inversion (*Ma et al., 2018*) and seismic interpretation (*Yuan et al., 2019a*).

Therefore, seismic data interpolation which can recover un-sampled data is an essential step in seismic data processing (*Yao and Jakubowicz, 2016*). In addition, seismic interpolation is the main method for verifying the quality of compressed sensing (CS)-based acquisition designs (*Mosher et al., 2017*; *Herrmann and Hennenfent, 2008*).

There exist four types of method for seismic interpolation:

1. The prediction filtering method that capable of interpolating regularly sampled aliased data (*Spitz, 1991*; *Parsani, 1999*).
2. The wave equation method that requires prior information of subsurface velocity models (*Ronen, 1987*; *Fomel, 2003*).
3. The sparsity-promoting method that can be further divided into fixed-basis based method (*Herrmann et al., 2000*; *Xu et al., 2005*; *Herrmann and Hennenfent, 2008*; *Cao and Zhao, 2017*) and learning-based method (*Liang et al., 2014*; *Zhou et al., 2014, 2015*). Some fixed-basis transforms have been proposed for interpolation of seismic data including the Fourier transform (*Abma and Kabir, 2006*; *Wang et al., 2016*), the Radon transform (*Herrmann et al., 2000*; *Gong et al., 2016*), the curvelet transform (*Candes et al., 2006*; *Herrmann and Hennenfent, 2008*; *Yang et al., 2013*; *Zhang and Chen, 2013*), the seislet transform (*Fomel and Liu, 2010*), and the dreamlet transform (*Wang et al., 2015*). The learning-based method takes advantage of machine learning to update tight-frame (*Liang et al., 2014*) or sparse dictionary (*Zhou et al., 2014, 2015*) which are data adaptive for seismic data expression. The learning-based method is computationally costly compared with the fixed-basis based method.
4. The rank reduction method which is based on the assumption that missing traces and random noise may increase the rank of a matrix or a tensor. This kind of method includes singular value decomposition (SVD) based method (*Oropeza and Sacchi, 2011*; *Kreimer and Sacchi, 2012*; *Gao et al., 2013*; *Sternfels et al., 2015*; *Chen et al., 2016*; *Zhang et al., 2017*) and SVD-free method (*Gao et al., 2015*).

Field seismic data always contain random noise during the process of seismic acquisition. The existence of random noise can seriously affect the performance of many interpolation methods, thus removing the noise in the sampled traces during interpolation is a challenging task. One method to treat noisy data interpolation is interpolation at first and denosing the interpolation result at second, but we have to do two treatments to get a noise-free complete seismic data. However, simultaneous interpolation and denoising which can realize interpolation and denoising in a unified framework can avoid the denoising processing. *Cao and Wang (2015)* proved that simultaneous interpolation and denoising can get comparable results to the interpolation-denoising process, thus simultaneous interpolation and denoising is more convenient and time-saving. There exist comprehensive studies on this research (*Oropeza and Sacchi, 2011*; *Gao et al., 2013*; *Cao and Wang, 2015*; *Chen et al., 2015*; *Wang et al., 2015, 2016*; *Zhang et al., 2017*). These methods are mainly the sparsity-promoting methods and the rank reduction methods. *Oropeza and Sacchi (2011)* proposed a multichannel singular spectrum analysis (MSSA) method to implement simultaneous seismic data denoising and interpolation. *Kreimer and Sacchi (2012)* described a tensor higher-order singular value decomposition (HOSVD) method for simultaneous noise-reduction and interpolation. Contrary to many multidimensional methods, the HOSVD method operates quite well in the presence of

curved events. *Gao et al. (2015)* developed a parallel matrix factorization (PMF) based method to solve 5D seismic data simultaneous reconstruction and denoising. *Zhang et al. (2016)* applied damped MSSA to simultaneous interpolation and denoising, and proposed a multi-step damped MSSA to improve its performance. *Chen et al. (2016)* developed a damped rank-reduction method for simultaneous denoising and reconstruction of 5D seismic data.

The projection onto convex sets (POCS) method is well-known for seismic interpolation because of its merits on computational efficiency and interpolation quality (*Abma and Kabir, 2006*). However, random noise in the sampled traces cannot be removed when using the POCS method (*Zhang and Chen, 2013*). Based on the idea of the POCS method, a weighted projection onto convex sets (WPOCS) method (*Gao et al., 2103*) was developed to overcome deficiencies of the POCS method by using a weighting factor. *Cao and Wang (2015)* proposed an improved projection onto convex sets (IPOCS) method which can remove random noise in the sampled traces when the minimum threshold values are chosen properly. *Wang et al. (2015)* derived a new weighted POCS method based on the dreamlet transform to achieve simultaneous seismic data interpolation and denoising. Recently, some researchers have developed joint low-rank and sparse inverse methods. *Sternfels et al. (2015)* developed a joint low-rank and sparse inversion strategy enabling the simultaneous attenuation of random and erratic noise with interpolation in pre-stack seismic data. *Zhang et al. (2017)* investigate multiple constraints for simultaneous seismic data reconstruction and denoising based on a novel hybrid rank-sparsity constraint (HRSC) model, which aims at combining the benefits of both sparsity-promoting transforms and rank reduction methods.

The POCS method cannot remove noise in the sampled traces and interpolation of the WPOCS method still contains noise in the sampled traces. We develop a modified thresholding method to overcome these deficiencies. The paper is organized as follows: we first present sparsity-promoting based noisy data interpolation models and methods. The mathematical model that the POCS method treat for is also given, and why the POCS method cannot solve noisy data interpolation is analyzed. We then proposed the modified thresholding method for noisy data interpolation. Based on the curvelet transform, two synthetic examples are presented to demonstrate the performance of the proposed method. In addition, one 2D filed data is used to compare the performances of the POCS method, the WPOCS method, the IPOCS method and the proposed method. The comparisons proved that the proposed thresholding method can obtain well performance for noisy seismic data interpolation.

2. METHODOLOGY

Assuming $\boldsymbol{\Phi} \in R^{M\times N}$ as the acquisition matrix, $\boldsymbol{d} \in R^{N}$ as the noise-free seismic data, $\boldsymbol{n} \in R^{M}$ as the additive noise, and $\boldsymbol{d}_{obs} \in R^{M}$ as the sampled seismic data, their relationship can be denoted as follows:

$$\boldsymbol{\Phi d} + \boldsymbol{n} = \boldsymbol{d}_{obs} . \tag{1}$$

The interpolation problem which involves obtaining $\boldsymbol{d}$ from $\boldsymbol{d}_{obs}$ and $\boldsymbol{\Phi}$ is ill-posed since the sampled seismic data are incomplete, i.e, $M < N$. Here M is the dimension of the sampled data $\boldsymbol{d}_{obs}$, and N is the dimension of the complete data $\boldsymbol{d}$ when they are arranged into vectors. Furthermore, the presence of noise may aggravate the ill-posedness of this problem. If $\boldsymbol{\Psi}$ denotes a transform such as the curvelet transform (*Candes et al., 2006*), and $\boldsymbol{x} = \boldsymbol{\Psi d}$ is sparse or compressible, Eq. (1) can be changed to

$$\mathbf{A}\boldsymbol{x} + \boldsymbol{n} = \boldsymbol{d}_{obs}, \tag{2}$$

where $\mathbf{A} = \boldsymbol{\Phi}\boldsymbol{\Psi}^{\mathrm{H}}$, and $\boldsymbol{\Psi}^{\mathrm{H}}$ is the inverse of $\boldsymbol{\Psi}$. In view of the sparsity of $\boldsymbol{x}$, a sparse optimization model can be established as follows:

$$\min \left\| \boldsymbol{x} \right\|_1 \quad \text{subject to } \left\| \mathbf{A}\boldsymbol{x} - \boldsymbol{d}_{obs} \right\|_2 \le \sigma, \tag{3}$$

where $\left\| \boldsymbol{x} \right\|_1$ is the L_1 norm of $\boldsymbol{x}$ and σ is the energy of the additive noise. Generally, the unconstrained form of problem (3) is more commonly used:

$$\min \frac{1}{2} \left\| \mathbf{A}\boldsymbol{x} - \boldsymbol{d}_{obs} \right\|_2^2 + \lambda \left\| \boldsymbol{x} \right\|_1, \tag{4}$$

where λ is the regularization parameter.

The thresholding method (*Daubechies et al., 2004*) is widely used to solve the L_1 norm regularized problems. As a thresholding method, the POCS method is computationally efficient (*Abma and Kabir, 2006*). However, it cannot remove random noise presented in the sampled traces (*Zhang and Chen, 2013*). The POCS method actually solves the following problem:

$$\min \left\| \boldsymbol{\Psi d} \right\|_1 \quad \text{subject to } \boldsymbol{\Phi d} = \boldsymbol{d}_{obs}. \tag{5}$$

In POCS, irregularly sampled data is taken to Fourier domain, then large amplitudes are kept using a thresholding operation, taking inverse FFT and coming back to (t, x) domain the initial recorded data are replaced, and this procedure is repeated for a few iterations, each time reducing the thresholding value.

The iterative formula of the POCS method (*Cao and Wang, 2015*) at the k-th iteration can be expressed as:

$$\boldsymbol{d}^{k+1} = \boldsymbol{d}_{obs} + \left(\mathbf{I} - \boldsymbol{\Phi} \right) \boldsymbol{\Psi}^{\mathrm{H}} T_{\tau_k} \left(\boldsymbol{\Psi d}^k \right) = P_{\left\{ d \mid \Phi d = d_{obs} \right\}} \left[\boldsymbol{\Psi}^{\mathrm{H}} T_{\tau_k} \left(\boldsymbol{\Psi d}^k \right) \right], \tag{6}$$

where $\boldsymbol{\Psi}^{\mathrm{H}} T_{\tau_k} \left(\boldsymbol{\Psi d}^k \right)$ is a predictive solution of $\boldsymbol{d}^k$, and $T_{\tau_k} \left(\cdot \right)$ denotes the soft thresholding operation, i.e., $T_{\tau_k} \left(s \right) = \operatorname{sgn}\left(s \right) \left(\left| s \right| - \tau_k \right)_+$ for a scalar s, τ_k is the k-th threshold value, and L is the maximum iteration number. In Eq. (6), $P_{\left\{ d \mid \Phi d = d_{obs} \right\}} \left[\boldsymbol{\Psi}^{\mathrm{H}} T_{\tau_k} \left(\boldsymbol{\Psi d}^k \right) \right]$ denotes the projection of $\boldsymbol{\Psi}^{\mathrm{H}} T_{\tau_k} \left(\boldsymbol{\Psi d}^k \right)$ onto

$\left\{\boldsymbol{d}\middle|\boldsymbol{\Phi d}=\boldsymbol{d}_{obs}\right\}$, which is a convex set. The projection is a reinsert or imputation process for the interpolation problem. Therefore, random noise in the observed traces cannot be removed using the POCS method. The iterative step of the WPOCS method (*Gao et al., 2103*) is as follows:

$$\boldsymbol{d}^{k+1}=\alpha\boldsymbol{d}_{obs}+\left(\mathbf{I}-\alpha\boldsymbol{\Phi}\right)\boldsymbol{\Psi}^{\mathrm{H}}T_{\tau_k}\left(\boldsymbol{\Psi d}^{k}\right),\quad k=1,2,\ldots,L, \tag{7}$$

where $\alpha\in(0,1]$ is the weighting factor. The difference between Eq. (6) and Eq. (7) is that the latter contains a weighting factor which should be chosen based on the energy of the noise. The WPOCS method is identical to the POCS method when $\alpha=1$.

The iterative format of the IPOCS method (*Cao and Wang, 2015*) can be expressed as follows:

$$\boldsymbol{d}^{k+1}=\boldsymbol{\Psi}^{\mathrm{H}}T_{\tau_k}\left\{\boldsymbol{\Psi}\left[\boldsymbol{d}_{obs}+\left(\mathbf{I}-\boldsymbol{\Phi}\right)\boldsymbol{d}^{k}\right]\right\},\quad k=1,2,\ldots,L, \tag{8}$$

where the thresholding operation is implemented after the projection operation in each iteration. Actually, this method is not a projection method since the projection is just an intermediate step in each iteration.

In order to improve performances of simultaneous interpolation and denoising, we proposed a modified thresholding method with the iterative frame as follows:

$$\boldsymbol{d}^{k+1}=\boldsymbol{\Psi}^{\mathrm{H}}T_{\tau_k}\left\{\boldsymbol{\Psi}\left[\boldsymbol{d}_{obs}+\kappa\left(\boldsymbol{d}_{obs}-\boldsymbol{\Phi d}^{k}\right)\right]\right\},\quad k=1,2,\ldots,L. \tag{9}$$

Here the initial solution $\boldsymbol{d}^{1}=0$, the initial threshold value is $\tau_1=\max\left\|\boldsymbol{\Psi d}_{obs}\right\|_{\infty}$, the minimum threshold value $\tau_{min}=\tau_L$ should be given according to the energy of noise, and $\tau_k=\tau_1\exp\left(\ln\left(\tau_1/\tau_L\right)\left[\left(k-1\right)/\left(L-1\right)\right]\right)$ is reduced exponentially; κ is a parameter between 0 and 1. Different from Eq. (8), the parameter κ is introduced to improve performances of simultaneous interpolation and denoising. In this equation, only one threshold value is needed to achieve simultaneous interpolation and denoising. $\boldsymbol{\Psi}$ is the curvelet transform (*Candes et al., 2006*), which has been used in seismic signal processing extensively. The curvelet transform is a local and directional decomposition of the data. The functions known as curvelets are used to decompose the original data in local components of various scales and dips. The discrete curvelet transform is an efficient implementation of the continuous curvelet transform. The directional properties of the curvelets are of great importance for seismic data sparse expression. The discrete curvelet transform is a tight frame, and synthesis operator is obtained using the adjoint transform. For more details about the curvelet transform, please refer to *Herrmann and Hennenfent (2008)* and *Cao et al. (2012)*. Based on the curvelet transform, the thresholding operator applies thresholding in all scales and directions with an unified parameter at each iteration.

To analyse the error of the interpolation quantitatively, the signal-to-noise ratio (*SNR*) is defined as

$$SNR = 10\log_{10}\frac{\left\|\boldsymbol{d}_{orig}\right\|_2^2}{\left\|\boldsymbol{d}_{orig}-\boldsymbol{d}_{int}\right\|_2^2},$$

where $\boldsymbol{d}_{orig}$ is the complete data and $\boldsymbol{d}_{int}$ is the interpolated data.

3. NUMERICAL EXAMPLES

In this section, the POCS, WPOCS, and IPOCS methods are used as benchmarks and all of these methods chosen the curvelet transform to represent seismic data sparsely (*Candes et al., 2006*). Figure 1a shows a simulated data containing 120 traces and 1000 time samples with sampling interval 4 ms. Simulated data from Fig. 1a with added noise are shown in Fig. 1b (*SNR* = 4.6278 dB). Figure 2a includes 50% of the traces shown in Fig. 1b based on the piece-wise sampling method (*Cao et al., 2012*). Figure 2b presents the interpolation result using the POCS method with an *SNR* of 7.2612 dB. Figure 3a presents the results of the WPOCS ($\alpha = 0.6$) interpolation with an *SNR* of 11.7386 dB. Figure 3b presents the interpolation using the proposed thresholding method ($\kappa = 0.9$) with an *SNR* of 15.8647 dB. The maximum number of iterations *L* for these methods is 60. The exponential reduction method for the threshold value is used for these methods because it is suitable for curvelet transform-based interpolation methods. The minimum threshold value τ_1 is very important for thresholding-based noisy data interpolation; thus,

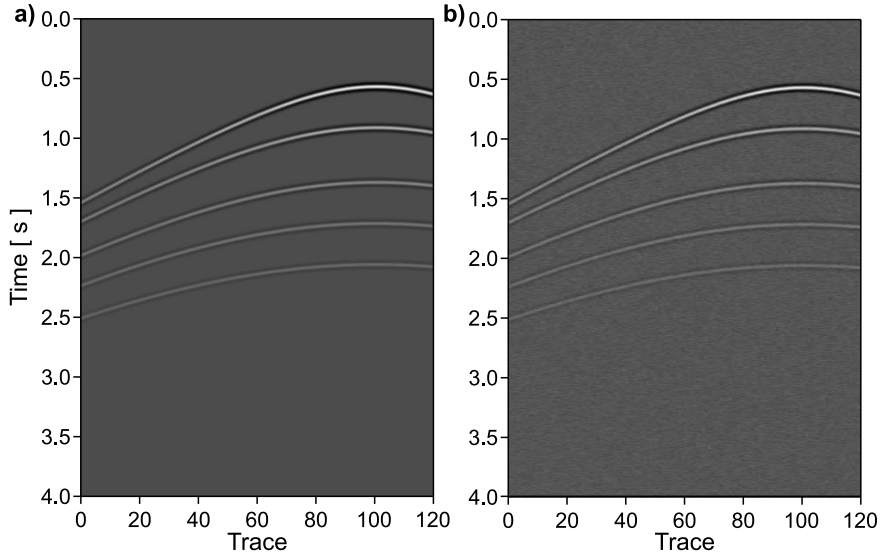

Fig. 1. **a)** Simulated 2D data; **b)** simulated 2D data with added noise (signal-to-noise ratio of 4.6278 dB).

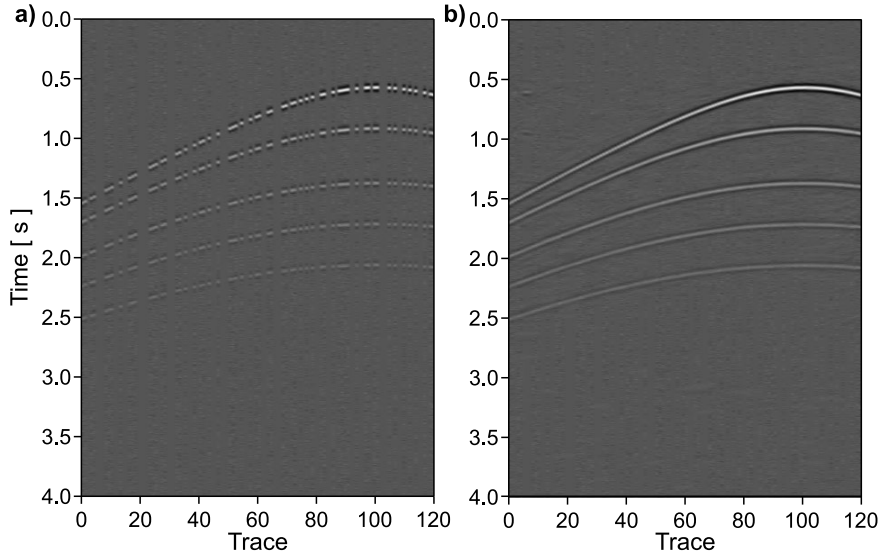

Fig. 2. **a)** Randomly sampled data from Fig. 1b with half of the traces missing; **b)** interpolation using the projection onto convex sets method with signal-to-noise ratio of 7.2612 dB.

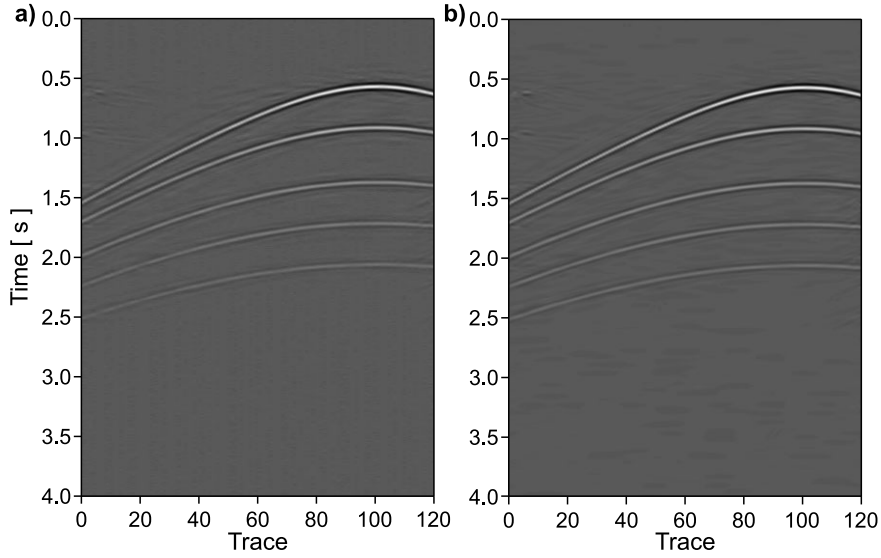

Fig. 3. **a)** Interpolation using the weighted projection onto convex sets (WPOCS) method (weighting factor $\alpha = 0.6$) with signal-to-noise ratio (*SNR*) of 11.7386 dB; **b)** interpolation using the proposed method (weighting factor $\kappa = 0.9$) with *SNR* = 15.6291 dB.

it should be chosen carefully. For this numerical test, the minimum threshold values of the POCS and WPOCS methods are both set as 0.031, and the minimum threshold value of the proposed method is 0.035. It should be emphasized that all the above parameters were chosen carefully.

Figure 4 shows comparison of these methods for two traces, trace 23 which was missing in the randomly sampled data, and trace 24 which was present in the randomly sampled data. The shown traces are from the initial data (true value), the noisy data, the POCS interpolated data, the WPOCS interpolated data, and the proposed method, respectively. For the missing trace (the 23-rd trace) interpolation, all three methods can generate acceptable results. For the sampled trace (the 24-th trace) interpolation, the POCS method is invalid and interpolation using the WPOCS method still contain noise; therefore, the interpolation results of the proposed method are the best among them.

Figure 5a shows a shot gather including 96 traces and 726 time samples. The time sampling rate is 4 ms. This data was obtained based on the Marmousi model (*Yao et al., 2016*), which has been widely used to test the efficiency of interpolation methods (*Yuan et al., 2019b*). Figure 5a with noise added is shown in Fig. 5b (*SNR* = 4.9731 dB). A sub-sampled version of Fig. 5b is shown in Fig. 6a with 58 randomly sampled traces. The POCS interpolation results are shown in Fig. 6b, with an *SNR* of 6.4250 dB. Figure 7a shows the WPOCS ($\alpha = 0.6$) interpolation results, with an *SNR* of 10.8388 dB. Figure 7b shows the interpolation results of the proposed method ($\kappa = 0.8$), with an *SNR* of 12.0173 dB. The minimum threshold values for the POCS, WPOCS, and the proposed method are 100, 60, and 90, respectively. The maximum number of iterations for these methods is 60.

Figure 8 shows comparison of these methods for two traces, trace 20 which was missing in the randomly sampled data, and trace 23 which was sampled in the randomly sampled data. The shown traces are from the initial data (true value), the noisy data, the

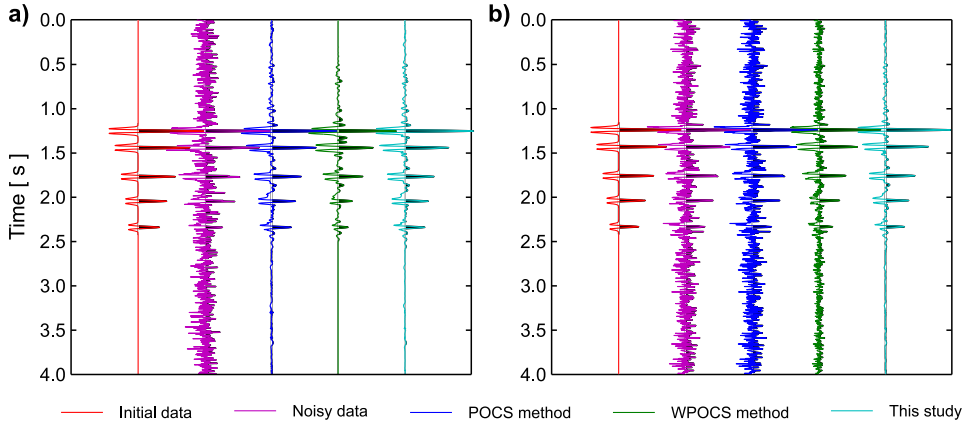

Fig. 4. **a)** Trace 23 and **b)** trace 24 of the simulated data. POCS: projection onto convex sets method, WPOCS: weighted POCS method.

POCS interpolated data, the WPOCS interpolated data, and the proposed method, respectively. It can be seen that the POCS method can realized missing trace interpolation but failed for sampled trace interpolation. Similar to the above example, the WPOCS

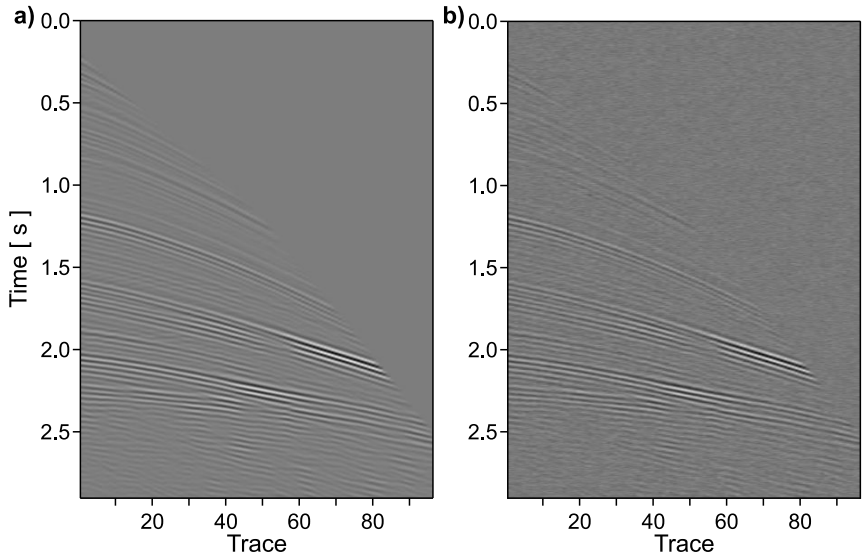

Fig. 5. **a)** The original Marmousi shot data; **b)** data with added noise with signal-to-noise ratio of 4.9731 dB.

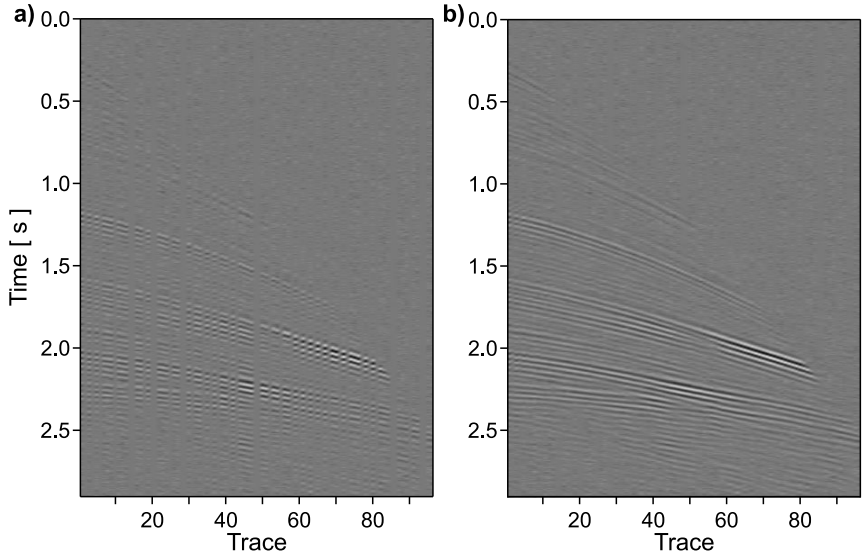

Fig. 6. **a)** Randomly sampled data from Fig. 5b; **b)** interpolation using the projection onto convex sets method (signal-to-noise ratio of 6.4250 dB).

method is better than the POCS method on noisy trace interpolation. Finally, interpolation using the proposed thresholding method can get better results than the POCS method and similar results to the WPOCS method after 60 iterations.

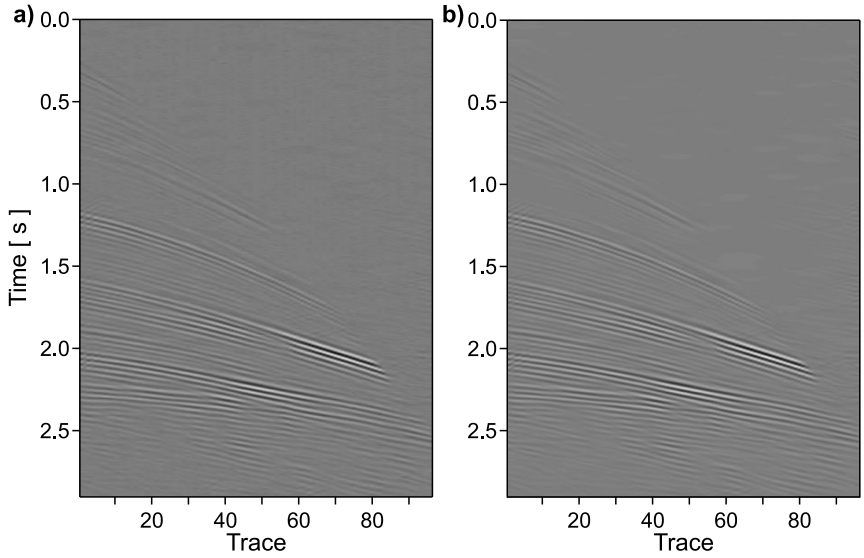

Fig. 7. **a)** Interpolation using weighted projection onto convex sets method (weighting factor $\alpha = 0.6$) with signal-to-noise ratio (*SNR*) of 10.8388 dB; **b)** interpolation using the proposed method (weighting factor $\kappa = 0.9$) with *SNR* = 12.0173 dB.

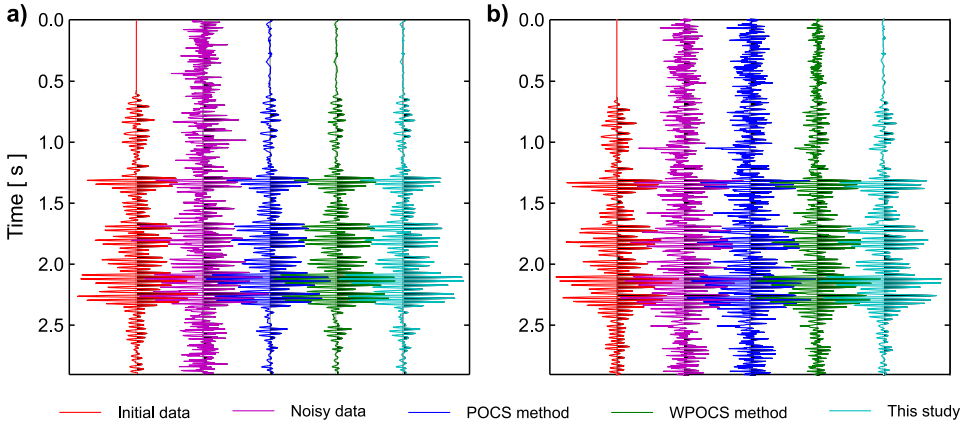

Fig. 8. **a)** Trace 20 and **b)** trace 23 of the Mrmousi data. POCS: projection onto convex sets method, WPOCS: weighted POCS method.

Figure 9a shows a field data set containing 128 traces and 700 time samples, gathered at a sampling rate of 4 ms. Figure 9b is a sub-sampled result of Fig. 9a, with 64 traces excluded. Figure 10a shows interpolation results of the WPOCS method ($\alpha = 0.6$) with

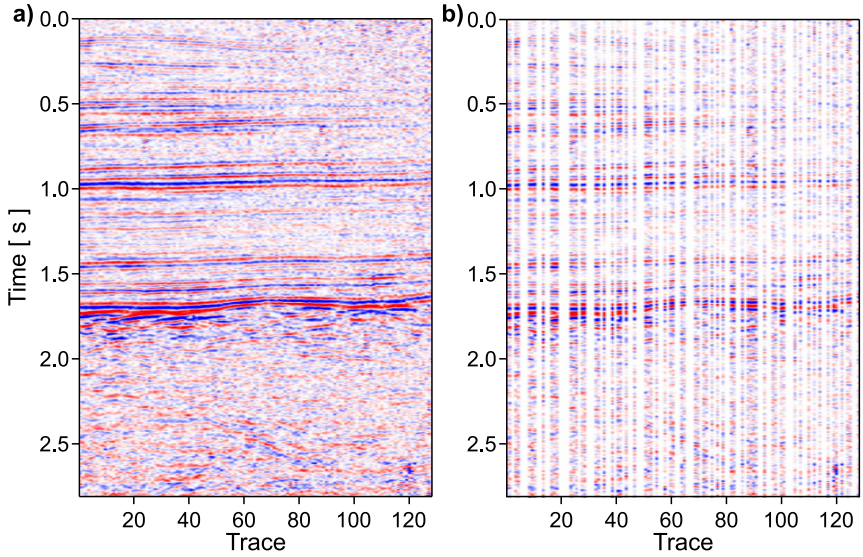

Fig. 9. **a)** Noisy field data; **b)** randomly sampled data with 64 traces excluded.

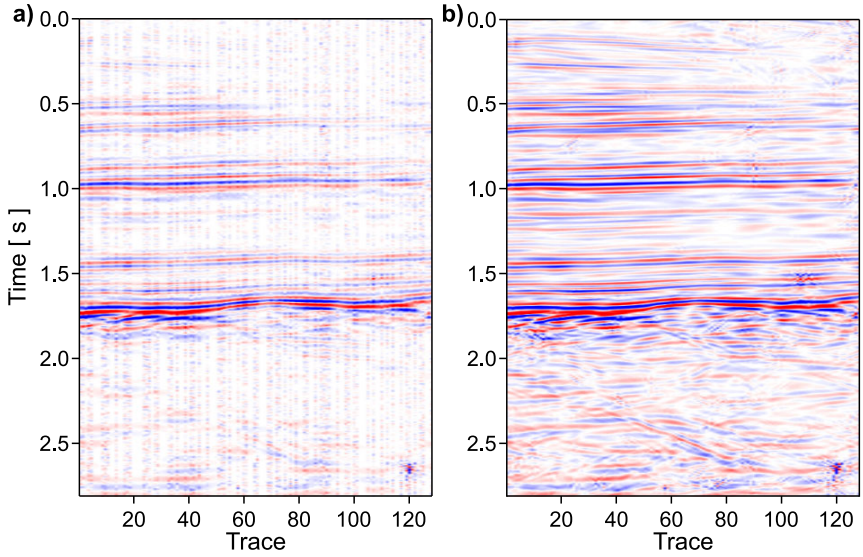

Fig. 10. **a)** Interpolation using weighted projection onto convex sets method (weighting factor $\alpha = 0.6$) with the maximum iteration number $L = 20$; **b)** interpolation using the proposed method (weighting factor $\kappa = 0.8$) with $L = 20$.

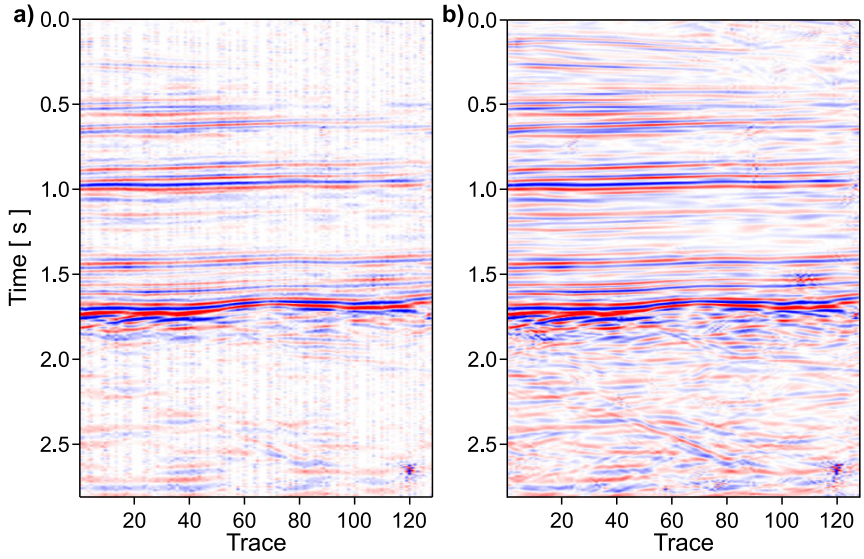

Fig. 11. The same as in Fig. 10, but with the maximum iteration number $L = 40$.

$L = 20$. Figure 10b is the interpolation results of the proposed method ($\kappa = 0.8$) with $L = 20$. The interpolation results of the WPOCS method ($\alpha = 0.6$) with $L = 40$ is shown in Fig. 11a. Figure 11b shows the interpolation results using the proposed method ($\kappa = 0.8$) with $L = 40$. For all these methods, the minimum threshold value is 0.05. Figure 12 shows comparison of their frequency-wavenumber (*f-k*) spectrum. It can be conclude that the proposed method can get better result than the WPOCS method on *SNR* when using the same iteration number. The proposed method after 20 iteration and 40 iteration get similar results.

4. CONCLUSIONS

This study proposes a thresholding based method for noisy data interpolation and analysed why the POCS method cannot be used to solve the problem of noisy data interpolation. Numerical experiments proved that acceptable results can be obtained using the POCS method for missing trace interpolation, but not for sampled noisy traces. The WPOCS method can reduce the energy of noise in the sampled traces and realize missing trace interpolation. The proposed thresholding method is valid not only for missing trace interpolation but also for sampled noisy trace interpolation. The proposed method can get better results than the WPOCS method when using the same iteration if the iteration number L is not large enough. The best results using the proposed method can be obtained when $\kappa = 0.8$ or 0.9. Finally, it should be noted that the quality of the results obtained using the WPOCS method and the proposed method depends on proper selection of the minimum threshold values τ_L, big τ_L should be chosen when the energy of the additive noise is large, and small τ_L corresponding to slight noise. The proposed method can also

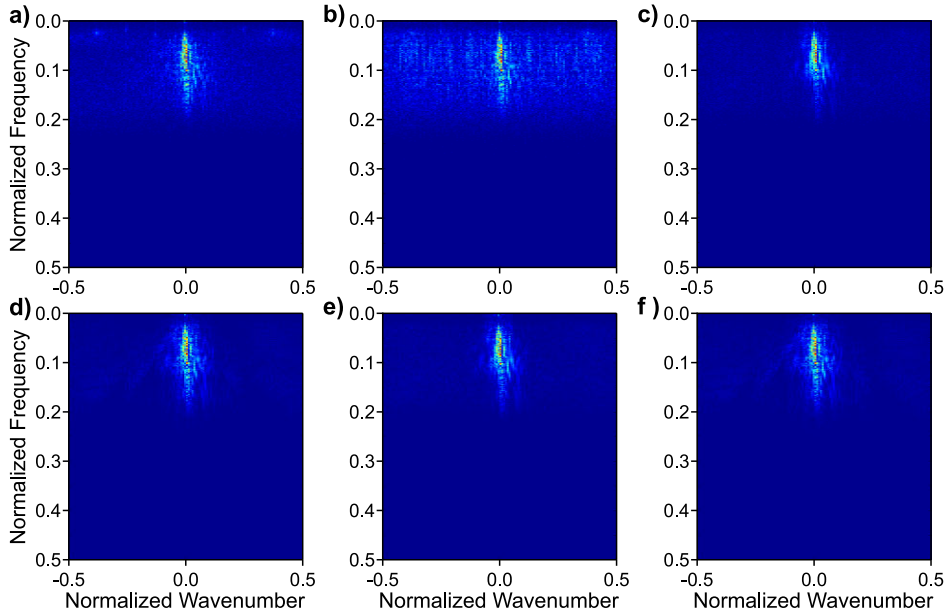

Fig. 12. Frequency-wavenumber spectrum of the field data: **a)** original noisy data; **b)** sampled data; **c)** result of the weighted projection onto convex sets method (WPOCS) method with data interpolated using the maximum iteration number $L = 20$; **d)** result of the proposed method with data interpolated using $L = 20$; **e)** the same as in c) but for $L = 40$; **f)** the same as in d), but for $L = 40$.

solve 3D data interpolation and denoising when 3D transforms are chosen to express seismic data sparsely. The minimum threshold values for simultaneous interpolation and denoising are presently manually determined which may cost lots of time. Future work will include finding adaptive methods to determine proper minimum threshold values.

Acknowledgments: The authors wish to thank F. Mahmoudian and three anonymous reviewers for greatly improving this manuscript. We thank the authors of CurveLab for providing access to their curvelet transform codes. This work was funded by National Natural Science Foundation of China (41674114, 41974116 and 41704120), Postdoctoral Research Foundation of China (2016M600171 and 2017T100137), Hundreds of Outstanding Innovative Talent Support Program for Colleges in Hebei Province (III) under grant number SLRC2017024, and Natural Science Foundation of Hebei Province under grant number D2017403027.

References

Abma R. and Kabir N., 2006. 3D interpolation of irregular data with a POCS algorithm. *Geophysics*, **71**, E91–E97.

Candes E., Demanet L., Donoho D. and Ying L., 2006. Fast discrete curvelet transforms. *Multiscale Model. Simul.*, **5**, 861–899.

Cao J. and Wang B., 2015. An improved projection onto convex sets methods for simultaneous interpolation and denoising. *Chinese J. Geophys.*, **58**, 2935–2947 (in Chinese).

Cao J., Wang Y. and Yang C., 2012. Seismic data restoration based on compressive sensing using the regularization and zero-norm sparse optimization. *Chinese J. Geophys.*, **55**, 596–607 (in Chinese).

Cao J. and Zhao J., 2017. Simultaneous seismic interpolation and denoising based on sparse inversion with a 3D low redundancy curvelet transform. *Explor. Geophys.*, **48**, 422–429.

Chen Y., Zhang D., Jin Z., Chen X.H., Zu S.H., Huang W.L. and Gan S.W., 2016. Simultaneous denoising and reconstruction of 5-D seismic data via damped rank-reduction method. *Geophys. J. Int.*, **206**, 1695–1717.

Daubechies I., Defrise M. and Mol C., 2004. An iterative thresholding algorithm for linear inverse problems with a sparsity constraint. *Commun. Pur. Appl. Math.*, **57**, 1413–1457.

Fomel S., 2003. Seismic reflection data interpolation with differential offset and shot continuation. *Geophysics*, **68**, 733–744.

Fomel S. and Liu Y., 2010. Seislet transform and seislet frame. *Geophysics*, **75**, V25–V38.

Gao J., Stanton A., Naghizadeh M., Naghizadeh M., Sacchi M. and Chen X., 2013. Convergence improvement and noise attenuation considerations for beyond alias projection onto convex sets reconstruction. *Geophys. Prospect.*, **61**, 138–151.

Gao J., Stanton A.and Sacchi M., 2015. Parallel matrix factorization algorithm and its application to 5D seismic reconstruction and denoising. *Geophysics*, **80**, V173–V187.

Gong X., Yu S. and Wang S., 2016. Prestack seismic data regularization using a time-variant anisotropic Radon transform. *J. Geophys. Eng.*, **13**, 462–469.

Herrmann F. and Hennenfent G., 2008. Non-parametric seismic data recovery with curvelet frames. *Geophys. J. Int.*, **173**, 233–248.

Herrmann P., Mojesky T., Magasan M. and Hugonnet P., 2000. De-aliased, high-resolution Radon transforms. *SEG Technical Program Expanded 2000*, 1953–1956.

Kreimer N. and Sacchi M., 2012. A tensor higher-order singular value decomposition for pre-stack simultaneous noise reduction and interpolation. *Geophysics*, **77**, V113–V122.

Liang J., Ma J. and Zhang X., 2014. Seismic data restoration via data-driven tight frame. *Geophysics*, **79**, V65–V74.

Ma M., Zhang R. and Yuan, S. Y., 2018. Multichannel impedance inversion for nonstationary seismic data based on the modified alternating direction method of multipliers. *Geophysics*, **84**, A1–A6.

Mosher C., Li C., Morley L., Ji Y., Janiszewski F., Olson R. and Brewer, J., 2014. Increasing the efficiency of seismic data acquisition via compressive sensing. *The Leading Edge*, **33**, 386–388.

Oropeza V. and Sacchi M., 2011. Simultaneous seismic data denoising and reconstruction via multichannel singular spectrum analysis. *Geophysics*, **76**, V25–V32.

Parsani M., 1999. Seismic trace interpolation using half-step prediction filters. *Geophysics*, **64**, 1461–1467.

Ronen J., 1987. Wave-equation trace interpolation. *Geophysics*, **52**, 973–984.

Spitz S., 1991. Seismic trace interpolation in the f-x domain. *Geophysics*, **56**, 785–794.

Smith P., Scott I. and Traylen T., 2012. Simultaneous time-lapse binning and regularization for 4D data. Extended Abstract. *74th EAGE Conference and Exhibition incorporating EUROPEC 2012*, DOI: 10.3997/2214-4609.20148240.

Sternfels R., Viguier G., Gondoin R. and Le Meur D., 2015. Multidimensional simultaneous random plus erratic noise attenuation and interpolation for seismic data by joint low-rank and sparse inversion. *Geophysics*, **80**, WD129–WD141.

Wang B, Wu R., Chen X. and Li J., 2015. Simultaneous seismic data interpolation and denoising with a new adaptive method based on dreamlet transform. *Geophys. J. Int*., **201**, 1182–1194.

Wang B., Chen X., Li J. and Cao J., 2016. An improved weighted projection onto convex sets methods for seismic data interpolation and denoising. *IEEE J. Sel. Top. Appl. Earth Observ. Remote Sens.*, **9**, 228–235.

Wang Y., Cao J. and Yang C., 2011. Recovery of seismic wavefields based on compressive sensing by an l l-norm constrained trust region method and the piecewise random subsampling. *Geophys. J. Int.*, **187**, 199–213.

Xu S., Zhang Y., Pham D. and Lambaré G., 2005. Antileakage Fourier transform for seismic data regularization. *Geophysics*, **70**, Z87–Z93.

Yang P., Gao J. and Chen W., 2013. On alaysis-based two-step interpolation methods for randomly sampled seismic data. Comput. Geosci., 51, 449-461.

Yao G. and Jakubowicz H., 2016. Least-squares reverse-time migration in a matrix-based formulation. *Geophys. Prospect*., **64**, 611–621.

Yao G., Silva N., Warner M. and Kalinicheva T., 2018. Separation of migration and tomography modes of full-waveform inversion in the plane wave domain. *J. Geophys. Res.-Solid Earth*, **123**, 1486–1501.

Yao G., Wu D. and Debens H., 2016. Adaptive finite difference for seismic wavefield modelling in acoustic media. *Sci. Rep.*, **6**, 30302, DOI: 10.1038/srep30302.

Yuan S., Su Y., Wang T., Wang J. and Wang S., 2019a. Geosteering phase attributes: A new detector for the discontinuities of seismic images. *IEEE Geosci. Remote Sens. Lett.*, **16**, 145–149.

Yuan S., Wang S., Luo Y., Wei W. and Wang G., 2019b. Impedance inversion by using the low-frequency full-waveform inversion result as a priori model. *Geophysics*, **84**, R149–R164.

Zhang D., Chen Y., Huang W. and Gan S., 2016. Multi-step damped multichannel singular spectrum analysis for simultaneous reconstruction and denoising of 3D seismic data. *J. Geophys. Eng*., **13**, 704–720.

Zhang D., Zhou Y., Chen H., Chen W., Zu S., and Chen Y., 2017. Hybrid rank-sparsity constraint model for simultaneous reconstruction and denoising of 3D seismic data. *Geophysics*, **82**, V351–V367.

Zhang H. and Chen X., 2013. Seismic data reconstruction based on jittered sampling and curvelet transform. *Chinese J. Geophys.*, **56**, 1637–1649 (in Chinese).

Zhou Y., Liu Z. and Zhang Z., 2015. Seismic signal reconstruction under the morphological component analysis frame-work combined with DCT and curvelet dictionary. *Geophys. Prospect. Petrol.*, **54**, 560–568.

Zhou Y., Wang L. and Pu Q., 2014. Seismic data reconstruction based on K-SVD dictionary learning under compressive sensing framework. *Oil Geophys. Prospect*., **49**, 652–660.